

Articles

Design, Synthesis, Potency, and Cytoselectivity of Anticancer Agents Derived by Parallel Synthesis from α -Aminosuberic AcidPia Kahnberg,^{†,‡} Andrew J. Lucke,^{†,‡} Matthew P. Glenn,^{†,‡} Glen M. Boyle,^{†,§} Joel D. A. Tyndall,[‡] Peter G. Parsons,[§] and David P. Fairlie^{*‡}*Centre for Drug Design and Development, Institute for Molecular Bioscience, University of Queensland, Brisbane, Queensland 4072, Australia, and Melanoma Genomics Group, The Queensland Institute for Medical Research, Herston, Queensland 4006, Australia*

Received March 9, 2005

Chemotherapy in the last century was characterized by cytotoxic drugs that did not discriminate between cancerous and normal cell types and were consequently accompanied by toxic side effects that were often dose limiting. The ability of differentiating agents to selectively kill cancer cells or transform them to a nonproliferating or normal phenotype could lead to cell- and tissue-specific drugs without the side effects of current cancer chemotherapeutics. This may be possible for a new generation of histone deacetylase inhibitors derived from amino acids. Structure–activity relationships are now reported for 43 compounds derived from 2-aminosuberic acid that kill a range of cancer cells, 26 being potent cytotoxins against MM96L melanoma cells (IC_{50} 20 nM–1 μ M), while 17 were between 5- and 60-fold more selective in killing MM96L melanoma cells versus normal (neonatal foreskin fibroblasts, NFF) cells. This represents a 10- to 100-fold increase in potency and up to a 10-fold higher selectivity over previously reported compounds derived from cysteine (*J. Med. Chem.* **2004**, *47*, 2984). Selectivity is also an underestimate, because the normal cells, NFF, are rarely all killed by the drugs that also induce selective blockade of the cell cycle for normal but not cancer cells. Selected compounds were tested against a panel of human cancer cell lines (melanomas, prostate, breast, ovarian, cervical, lung, and colon) and found to be both selective and potent cytotoxins (IC_{50} 20 nM–1 μ M). Compounds in this class typically inhibit human histone deacetylases, as evidenced by hyperacetylation of histones in both normal and cancer cells, induce expression of p21, and differentiate surviving cancer cells to a nonproliferating phenotype. These compounds may be valuable leads for the development of new chemotherapeutic agents.

Introduction

The 20th century saw a wide range of cytotoxic chemotherapies used to treat human cancer, the most effective being combinations of drugs (e.g., cyclophosphamide, fluorouracil, doxorubicin, and vincristine). Maximum therapeutic outcomes were obtained for synergistic combinations of drugs that had different mechanisms of cell killing and included antimetabolites (e.g., folate, purine, and pyrimidine antagonists), covalent DNA-binding drugs (nitrogen mustards, alkyl sulfonates, aziridine derivatives, and platinum complexes), noncovalent DNA-binding drugs (anthracyclines and bleomycins), inhibitors of chromatin function (topoisomerase and microtubule inhibitors), regulators of endocrine function (glucocorticoids and anties-

trogens), and angiogenesis inhibitors, to name a few. Typically, such antitumor agents were nonselective cytotoxins, killing normal cells along with tumor cells and, consequently, resulted in side effects that were often cumulative and dose limiting.

An important goal of the early 21st century cancer medicine is the development of selective cancer chemotherapeutics that specifically destroy malignant tumors without damaging normal tissues. A promising approach toward this objective^{1–4} is the use of differentiating agents that can selectively affect tumor growth, either by killing cancer cells or transforming them to a nonproliferating or more normal phenotype. Such an approach has the potential to be tissue-specific and to avoid the side effects of current drugs. Among early compounds known to differentiate cancer cells in cell culture were histone deacetylase inhibitors like butyrate, retinoic acid, HMBA, ABHA, SBHA, SAHA, scriptaid, sirtinol, and so on,^{5–9} which were all of low potency, not very selective *in vivo*, and differentiation was usually reversible. More potent HDAC inhibitors that have shown more promising anticancer properties *in vitro* include trichostatin (**1**),^{10,11} trapoxin (**2**),¹² apicidin,¹³ and analogues.^{1,14–18} Such compounds are typically cytotoxic to both normal and cancer cells and are ineffective *in vivo* due to low bioavailability and rapid metabolism. Up to a 5:1 selectivity in killing cancer cell types over normal cell types has been observed, for example, for **1**, suggesting that a more intensive study of HDAC inhibition

* Corresponding author: Phone: +61-7-33462989. Fax: +61-7-33462990. E-mail: d.fairlie@imb.uq.edu.au.

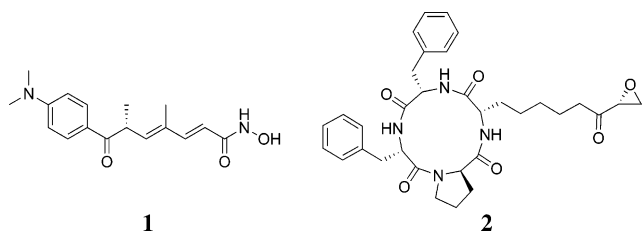
[†] These authors contributed equally.

[‡] University of Queensland.

[§] The Queensland Institute for Medical Research.

^a Abbreviations: Ac, acetyl; DCM, dichloromethane; DIPEA, diisopropylethylamine; DMBA, 1,3-dimethylbarbituric acid; DMF, dimethylformamide; DMSO, dimethyl sulfoxide; EtOAc, ethyl acetate; Fmoc, 9H-fluoren-9-ylmethoxycarbonyl; Fmoc-OSu, 9-fluorenylmethyloxycarbonyl-N-hydroxysuccinimide; HATU, O-(7-azabenzotriazol-1-yl)-1,1,3,3-tetramethyluronium hexafluorophosphate; HBTU, [(benzotriazolyl)oxy]-N,N',N',N'-tetramethyluronium hexafluorophosphate; rpHPLC, reversed phase high performance liquid chromatography; LRMS, low-resolution mass spectroscopy; Pro, proline; TFA, trifluoroacetic acid; THF, tetrahydrofuran.

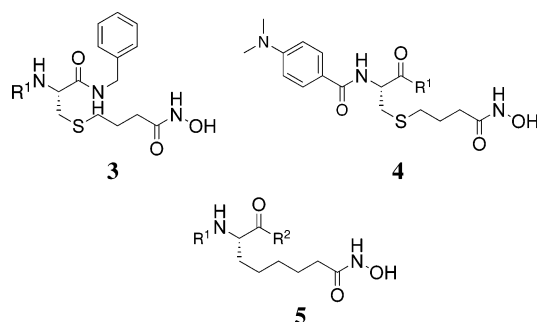
might lead to potent antitumor agents with even higher selectivity for cancer cell lines. More recently, it was reported that a cinnamic acid based HDAC inhibitor NVP-LAQ824 had some selective toxicity toward cancer cell lines, while inducing growth arrest in normal fibroblasts.¹⁹



There are 18 human genes known²⁰ to encode histone deacetylase enzymes (HDACs) and eleven HDACs have been isolated and identified to date. They can be divided into two classes based on their similarity to the yeast histone deacetylases²¹ Rpd3 (class I, HDAC1–3 and 8) and Hda1 (class II, HDAC4–7 and 9–11). The two classes share a highly conserved catalytic domain of amino acids, but class II proteins are two to three times larger in size than class I. While limited structural information is available for these human proteins, an X-ray crystal structure of a bacterial HDAC (HDLP, 1c3r) has been solved in complex with the HDAC inhibitor **1**.²² HDLP shares ~32% homology with HDAC1, deacetylates histones *in vitro*, and is inhibited by known HDAC inhibitors.²² There is high sequence homology between the bacterial and the human HDACs within the catalytic core of the enzyme, which the crystal structure reveals to be an ~11 Å deep hydrophobic tube that narrows to ~4 Å at the active site and contains a catalytic divalent zinc cation, water molecule, and histidine-aspartate charge-relay system. Most of the residues in the HDLP structure that interact directly with **1** are highly conserved among all the HDACs, but there is less conservation in adjoining residues and considerable differences between the HDAC classes. Most notably, there is significant deviation on the enzyme surface, which has a number of shallow pockets adjacent to the deep active site pocket. The considerable diversity within this region suggests that it should be possible to develop specific inhibitors of each of the known HDACs. Recently, two reports appeared on the crystal structure of human HDAC8 complexed with a variety of hydroxamic acid inhibitors.^{23,24} These crystal structures suggest that the active site of HDAC8 is more malleable than that of the HDLP crystal structure, containing structural variability in loop regions about the active site surface.

Current HDAC inhibitors in clinical trials are regarded as broad spectrum HDAC inhibitors with moderate anticancer effects that are well tolerated. Ultimately, it would be desirable clinically to have much more potent anticancer drugs that are well tolerated. Of various approaches to achieve this, one is to produce inhibitors that are specific for a particular HDAC that is overexpressed in cancer. However, the specific HDAC enzyme inhibition approach to develop HDAC inhibitors has to date been problematic, as commercially available HDAC assay kits have previously been mixtures of class I HDACs, recombinant expression of individual HDACs was difficult and expensive to commercially exploit, and cell/tissue distributions of HDACs remain unknown.²⁵ A second approach which we have employed here is to use cell-based antiproliferative assays to screen for drugs that are both selective and potent cancer cell killers relative to normal cells. Furthermore, by screening a range of cancer cell lines, tumor-selective drugs may be found that may in turn be more selective for HDAC enzymes

overexpressed in a particular cancer cell line. Class II HDACs are found in both the nucleus and the cytoplasm and have been shown to be more tissue specific in some cases. This observation may enable the SAR of HDAC inhibitors to be potentially examined by antiproliferative cytoselectivities over a range of differing tissue specific cancer cell lines.



Recently, we investigated²⁶ structure–activity relationships for two classes of L-cysteine-derived anticancer agents (e.g., **3** and **4**) with combinatorial variations at the N- and C-termini of cysteine. Some of those compounds were orally active and cytotoxic at ~100 nM concentrations against various cancer cell lines, with cytoselectivities of up to 6:1 for cancer cells over normal cells. We wondered, however, whether the two C–S bonds in those compounds, being longer than the analogous C–C bonds in lysine side chains of natural HDAC substrates, might provide too much conformational freedom to the enzyme-bound inhibitor at the rim of the tubular active site. The consequence of pushing the inhibitor branch point (the chiral carbon) further from the tubular enzyme active site entrance might diminish inhibitor interactions at the surface. We therefore decided to reduce the freedom of the bound inhibitor at the rim of the active site by replacing –S– with –CH₂– to more closely mimic the L-lysine side chain, while maintaining the analogous *S*-stereochemistry. Herein, we report a structurally diverse series of aliphatic analogues like **5**, designed with the aid of a homology model and synthesized using enzymatic enantioselection. Some of these compounds show higher potencies (10–100-fold higher) and higher selectivities (up to 10-fold higher) than **3** or **4** in killing cancer cells of various types. The aminosuberlic acid component of **5** has now been used as a template to undertake structure–activity studies of anticancer potency and cytoselectivity. This work represents an important step toward more selective chemotherapeutics that might either specifically destroy malignant tumors without damaging normal tissues or selectively differentiate cancer cells to a nonproliferating phenotype, an approach that has the potential to be tissue-specific and to avoid side effects of current anticancer drugs.

Results and Discussion

Model of Histone Deacetylases. Based on sequence homology, most human histone deacetylases are either in class I (HDAC1–3, 8) or Class II (HDAC4–7, 9).²⁷ Both classes have an essentially conserved catalytic domain, but class II enzymes are substantially larger than class I and their catalytic domain is at the C-terminus of the protein. HDACs 10²⁸ and 11²⁹ have also been categorized as class 2 and, while similar to one another, differ from the other HDACs. HDAC11 has its catalytic domain at the N-terminus of the protein. HDAC10 has similar sequence homology to HDAC6 but is larger (669 residues). Sirtuin deacetylases make up class 3, while a group of new proteins are class 4, though similar to human HDAC11.³⁰

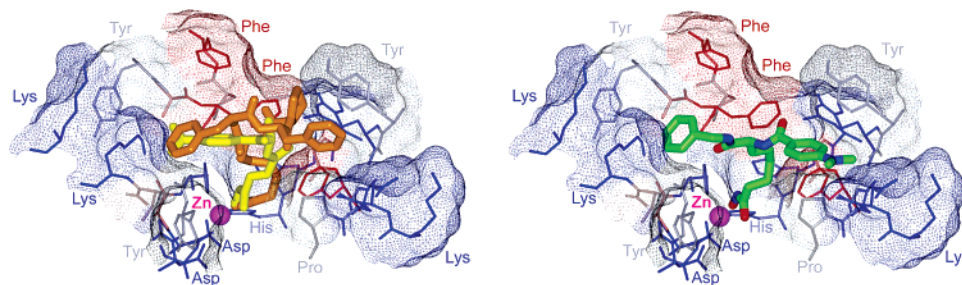


Figure 1. HDAC1 homology model. Lowest energy GOLD docked conformations of (left) TSA (yellow), trapoxin B analogue (orange), and (right) hydroxamic acid **6** (colored by atom type) in the solvent-accessible active site of the HDAC1 homology model (colored by hydrophobicity: red hydrophobic to blue hydrophilic).

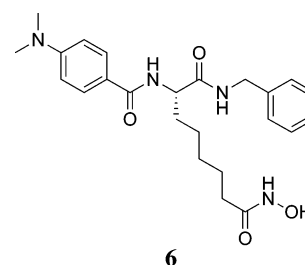
When the present work reported herein was conducted, there were no crystal structures for human HDAC enzymes, so a homology model of HDAC1 was created based on alignment of sequences of class I HDACs. The model was then used in docking studies on known and potential new HDAC inhibitors that were designed *in silico*. Subsequently, a crystal structure of human HDAC8 complexed with TSA has appeared.²³ The homology model and the crystal structure of human HDAC8 were structurally aligned with an overall backbone rmsd of 0.50 Å, indicating high structural similarity. The greatest variability between the two structures occurred at the surface active site loop regions, as expected, so the homology model used in the docking studies herein is retrospectively considered to be valid.

Inhibitor Design. Trichostatin (**1**) was initially docked into the active site of our HDAC1 homology model using a genetic docking algorithm (GOLD)³¹ and two tight binding conformations were identified. These conformations differ most notably in the position of the dimethyl aminobenzoyl group, which can dock into either of two shallow surface pockets adjacent to the deep active site pocket. One of these conformations (Figure 1) is very similar to the enzyme bound conformation of **1** observed in the HDLP crystal structure.²² In both conformations, zinc coordination to the hydroxamic acid was observed in addition to hydrophobic interactions between the rigid diene and the deep tubular cavity.

The naturally occurring cyclic tetrapeptide HDAC inhibitor trapoxin B (**2**) was modified to include a hydroxamic acid zinc binding group in place of the epoxy-ketone found in the natural product. That cyclic tetrapeptide was synthesized in house and found to be a potent killer of melanoma cells (MM96L, IC₅₀ ~ 30 nM). A randomized conformational search (Macromodel³²) of the cyclic tetrapeptide identified the most stable conformation to incorporate a bis- γ -turn, essentially identical to the established solution structures³³ of related cyclic tetrapeptides. This conformation was docked into the HDAC1 homology structure using GOLD (Figure 1). Tight binding conformations were identified that placed the Phe side chains in contact with the shallow pockets of the enzyme surface. The positions of these aromatic side chains were very similar to those observed for the dimethylaminobenzoyl group of **1** (Figure 1). The side chain of Pro is accommodated by a smaller pocket and may primarily be involved in stabilization of the tetrapeptide conformation.

The Phe side chains of **2** are presumably important foliage on the cyclic tetrapeptide scaffold for tight enzyme binding because related naturally occurring cyclic tetrapeptide inhibitors include similar hydrophobic groups (Phe, Trp, Tyr) at these positions. Optimization of these surface interactions offers the greatest possibility of identifying features that deliver HDAC selectivity. It was envisaged that a tripeptide analogue incorporating similar groups to those observed in the potent naturally occurring cyclic tetrapeptide inhibitors (hydrophobic, aromatic,

and basic) could span across **2** and allow functional mimicry of these surface interactions using a greatly simplified system.

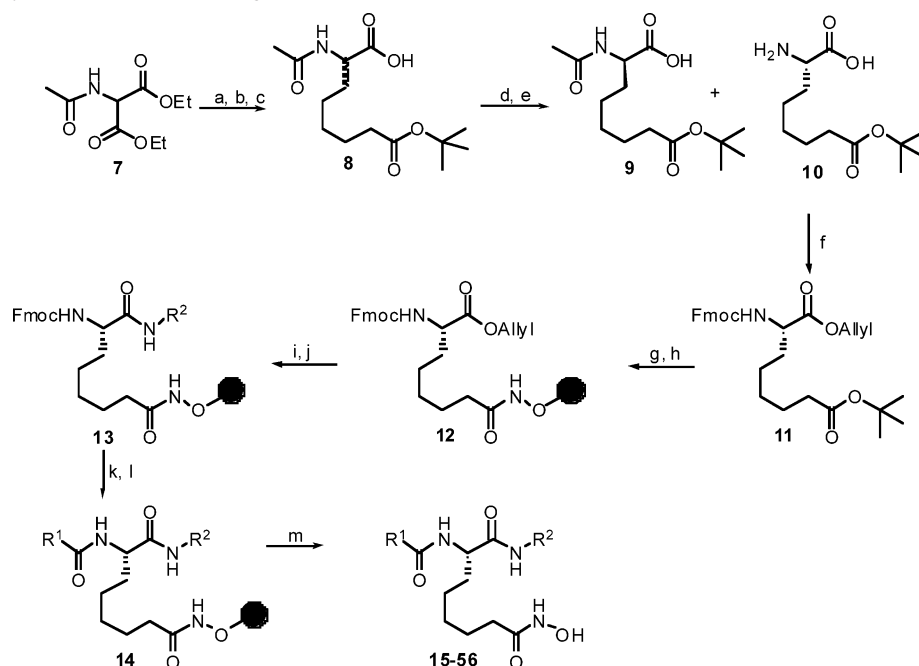


To test the validity of this approach, we examined a hybrid of **1** and **2**, namely, **6**, and docked it into the homology structure. This incorporates the dimethyl aminobenzoyl and hydroxamic acids groups of **1**, a benzyl substituent similar to the Phe side chain of **2**, a pentamethylene aliphatic side chain extending from the chiral carbon of the amino acid to the putative zinc-binding hydroxamate. Tight binding conformations were identified that closely mimicked those observed for the hydroxamate analogue of **2** (Figure 1). The aromatic groups projected into the shallow surface pockets of the enzyme and suggested numerous potential hydrogen bonding, ionic, and hydrophobic interactions that could be accessed from this general model. We, therefore, decided to synthesize compound **6** and analogues that varied the amide terminal substituents. After most of the work below had been completed, the *R*-enantiomer of **6** (compound **15**) was also docked into the homology model using GOLD, and **15** was surprisingly found to have a slightly higher Gold Fitness score (65.9 vs 68.6, respectively). Compound **15** made better H-bonding and Van der Waals interactions with the homology enzyme structure, indicating the potential for conceivably more potent enzyme inhibition and enhanced killing of cancer cells *in vitro*.

Before synthesis of the hydroxamic acid analogues was performed, the predicted lipophilicity was calculated *in silico* at pH 7 (log *D* 7.0 being the octanol/water partition coefficient) using PALLAS,³⁴ with one compound having a log *D* 0–1, 27 compounds with log *D* 1–3, and sixteen compounds with log *D* 3–5, in anticipation of suitable penetration of cell membranes.

Parallel Synthesis of Inhibitors. Alkylation of acetamido malonate **7** with 6-iodo-hexanoic acid *tert*-butyl ester, and subsequent hydrolysis afforded 2-acetylamino-octanedioic acid 8-*tert*-butyl ester **8**, Scheme 1. Chiral resolution was achieved through the known enzymatic treatment of the racemic mixture of **8** with acylase I from *aspergillus melleus*, which selectively deacetylated the 2*S*-enantiomer (~24 h), after which the 2*R*-enantiomer was deacetylated at a greatly reduced rate. Workup of the reaction after 24 h provided a 1:1 mixture of 2*R*-acetamide **9** and 2*S*-amine **10**. Amine **10** was protected with Fmoc-OSu

Scheme 1. Parallel Synthesis of Antitumor Agents Based on HDAC Inhibition



Reagents and conditions: (a) (1) NaH, DMF; (2) 6-iodo-hexanoic acid *tert*-butyl ester; (b) LiCl-H₂O, DMSO, 160 °C; (c) LiOH, H₂O/EtOH; (d) acylase I (*Aspergillus melleus*), CoCl₂, phosphate buffer pH 7.2; (e) (1) Fmoc-OSu, NaHCO₃, THF/H₂O; (2) rpHPLC separation; (f) allyl bromide, NaHCO₃, DMF; (g) TFA/DCM 9:1; (h) 2-(9*H*-fluoren-9-ylmethoxycarbonylamino)-octanedioic acid 1-allyl ester, 2-chlorotriethylhydroxylamine resin, HATU, DIPEA, DMF; (i) PdP(Ph)₃, DMBA, DCM; (j) R² = acid, HBTU, DIPEA, DMF; (k) piperidine/DMF; (l) R² = amine, HBTU, DIPEA, DMF; (m) TFA/DCM 95:5.

under basic conditions, and the two enantiomers were readily separable by rpHPLC. After separation, recovered acetamide **9** was hydrolyzed, and the resulting free amine was protected with Fmoc-OSu, providing access to both enantiomers for the remainder of the synthesis (Scheme 1). Compounds **15** and **16–23** (racemic derivatives) were synthesized in a similar manner utilizing a modified protection strategy (Supporting Information).

Free acid **10** was protected as an allyl ester, yielding fully protected compound **11**. TFA was used to selectively remove the *tert*-butyl protecting group from **11**, and the resulting acid was coupled to chlorotriethylhydroxylamine resin to yield resin-bound intermediate **12**. Deprotection of the allyl ester **12** and coupling of the appropriate amine gave derivative **13** on resin. Removal of the Fmoc protecting group, followed by coupling of a variety of acids, gave derivatives **14** on resin. Cleavage from resin with 5% TFA in DCM produced hydroxamic acids **6** and **15–56**, which were purified by rpHPLC and characterized by mass spectrometry and ¹H NMR spectroscopy.

Antiproliferative Activity Against MM96L Melanoma Cells. Cytotoxicity of 44 α -aminosuberic acid derived hydroxamic acids (**6**, **15–57**) was determined by clonogenic survival of human cancer cells (MM96L and melanoma) and human normal cells (NFF and neonatal foreskin fibroblasts), as described previously.²⁶ Twenty-seven compounds were potent cytotoxins against MM96L melanoma cells, including compounds **15–19**, **24**, **26**, **29**, **32**, **33**, **36**, **37**, **39–41**, **44**, **46–49**, and **51–56**, with IC₅₀ < 1 μ M. Six of these compounds, **47**, **51–53**, **55**, and **56**, were an order of magnitude more potent (IC₅₀ 20–80 nM) than the rest and of comparable potency to **1**. This contrast with the very best of our previously reported cysteine-derived compounds,²⁶ which had IC₅₀ ~ 0.2 μ M and little selectivity SI < 6.

Previously, we had shown that cysteine-derived antitumor agents, like **3** and **4**, had decreased potency with flexible alkyl substituents at the R¹ and R² positions.²⁶ Therefore, we chose to examine predominantly aromatic side-chain substituents that

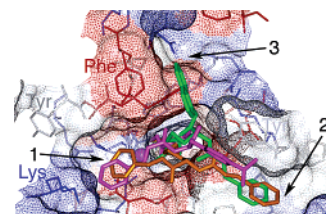


Figure 2. Highest ranked GOLD docked conformations of **26** (orange), **39** (purple), and **53** (green) in the solvent-accessible active site of the HDAC1 homology model (colored by hydrophobicity: red hydrophobic to blue hydrophilic) with three binding pockets indicated.

were less flexible at positions R¹ and R². The five most potent compounds with IC₅₀ < 50 nM (**51–53**, **55**, and **56**) all have a rigid bulky 8-aminoquinoline substituent at the R² position with aromatic groups; dimethylamino benzoic acid **51**, 2-indole carboxylic acid **52**, *trans* cinnamic acid **53**, or carbamate substituents; benzyl carbamate **55** or isobutyl carbamate **56** at R¹. These groups provide short rigid aromatic groups to bind into the hydrophobic pocket at the R¹ position. Substitution of the smaller, more flexible benzyl amine for 8-aminoquinoline at R² gave a 2–80-fold loss in potency.

Twenty-one compounds (**6**, **15**, **16**, **18**, **21**, and **23–38**) contain a benzylamine substituent at R², with a variety of aromatic groups at R¹. Compounds with IC₅₀ < 1 μ M were *para*-substituted aromatic derivatives such as 4-dimethylamino **15** and **16**, 4-trifluoromethyl **32**, but not 4-nitro **23** or 4-bromo **25** benzoic acids. Heterocyclic aromatic substituents at R¹ such as 2-furan **18**, 2-thiophene **29**, bulkier 2-indole **24**, **36**, **37**, carboxylic acids, and 3-indolacetic acid **33** were all potent (IC₅₀ < 1 μ M) cytotoxins against MM96L cells. However, introduction of flexibility to the side chain with two or more carbon atoms between the carbonyl carbon and the aromatic heterocycle (e.g., **34** and **38**) resulted in a loss of potency. Compounds **28**, **30**, and **35** contain bulky aromatic substituents at R² and are less potent than the simpler aromatic substituents, such as in **15** and **24**. Replacing the benzyl amine group at R¹ with

Table 1. Structure–Activity Relationships of Antitumor Agents

No.	R1	R2	*	log D	IC ₅₀ (μM) ^a NFF	IC ₅₀ (μM) ^a MM96L	SI ^b	No.	R1	R2	*	log D	IC ₅₀ (μM) ^a NFF	IC ₅₀ (μM) ^a MM96L	SI ^b
1	-	-		2.5	0.20	0.03	6.7	36			S	3.3	1.94	0.49	4.0
6			S	2.8	12	1.6	7.8	37			S	2.0	2.21	0.33	6.7
15			R	2.8	1.0	0.16	6.0	38			S	2.9	10.4	3.24	3.2
16			rac	2.8	0.87	0.13	6.7	39			S	2.3	0.24	0.16	1.5
17			rac	3.6	1.81	0.3	6.0	40			S	2.8	0.65	0.61	1.1
18			rac	1.1	4.6	0.2	23	41			S	3.6	0.40	0.22	1.8
19			rac	1.3	1.3	0.97	1.3	42			S	1.9	33	3.6	9.1
20			rac	1.0	4.4	1.5	2.9	43			S	1.9	2.09	1.15	1.8
21			rac	1.2	24	9.5	2.5	44			S	1.8	5.24	0.83	6.3
22			rac	1.0	12	9	1.3	45			S	1.2	23.3	4.32	5.4
23			rac	0.9	9	6	1.5	46			S	4.8	2.2	0.33	6.7
24			S	2.5	1.26	0.25	5.0	47			S	5.3	0.19	0.07	2.5
25			S	3.0	5.86	1.99	4.2	48			S	4.1	3.0	0.9	3.5
26			S	2.7	4.01	0.46	8.7	49			S	3.4	1.6	0.9	1.7
27			S	3.1	7.13	3.95	1.8	50			S	2.9	1.7	1.7	1
28			S	4.0	5.13	2.36	2.2	51			S	2.8	0.57	0.02	28
29			S	2.0	5.20	0.89	5.8	52			S	2.9	0.337	0.021	16
30			S	4.5	5.37	3.2	1.7	53			S	3.2	1.24	0.021	59
31			S	2.5	1.52	1.52	1	54			S	3.8	0.696	0.258	2.7
32			S	3.3	1.61	0.66	2.4	55			S	2.9	0.452	0.043	10.5
33			S	2.3	>2.2	0.33	>7	56			S	2.6	0.081	0.023	3.5
34			S	3.3	7.03	1.85	3.8								
35			S	3.3	9.8	NA ^c									

analogous pyridine derivatives **42–45** gave compounds with slightly less potency, except for **44**, which is approximately twice as potent as **25**. The *R*-enantiomer **15** was surprisingly found to be 10 times more potent than the corresponding *S*-enantiomer **6**. The increased potency of **15** compared to **6** is consistent with the GOLD docking results, which showed that **15** made slightly better H-bonding and van der Waals interactions with the homology model of the enzyme HDAC1 than **6**. This was an intriguing result and indicated that compounds derived from *D*-amino acids might provide even more potent and stable *in vivo* anticancer compounds. We are examining antiproliferative and cytoselectivity properties of *R*-enantiomers and will report the results in a future publication.

Docking of TSA (**1**) and trapoxin B (**2**) into the homology model of HDAC1 identified three surface binding pockets. The two larger surface pockets were filled with either the dimethyl aminobenzoyl group of **1** or the Phe side chains of **2**. The third, smaller pocket was filled by the Pro side chain of **2** and was not expected to be targeted by our compounds. However, subsequent docking of a selection of compounds after the *in vitro* trials indicated that the smaller pocket may be important for potency and selectivity. This was illustrated by docking cinnamic acid derivatives **26**, **39**, and **53** (Figure 2), with these compounds having IC₅₀ values of 460, 160, and 21 nM toward MM96L cancer cells and SI values of 8.7, 1.5, and 59 respectively (Table 1). Compound **26**, with moderate potency

Table 2. Comparative Antiproliferative Potencies of **16** against 17 Different Human Cancer Cell Lines vs a Normal Cell Line (NFF)

cell line ^a	IC ₅₀ (μM)	SI
MM96L	0.13	6.7
MM229	0.60	1.5
MM329	0.06	14.5
MM470	0.09	9.7
MM604	0.01	87
Mel RM	0.95	0.9
Mel FH	0.08	10.9
SK-Mel-28	0.06	14.5
DO4	0.12	7.3
D14	0.26	3.3
D11	0.3	2.9
D17	0.06	14.5
LSP M2	0.45	1.9
AF-6	0.30	2.9
AO7 RM	0.18	4.8
A2058	0.10	8.7
HeLa	0.09	9.7
NFF	0.87	1

^a MM96L, MM229, MM329, MM470, MM604, Mel RM and FH, SK-Mel-28, DO4, D11, D14, D17, LSP M2, AF-6, A07, A2059, melanoma; HeLa, cervical carcinoma; NFF neonatal foreskin fibroblasts.

and selectivity, docked into the homology model with the benzylamine group in pocket 1 (Figure 2) and the cinnamyl substituent in pocket 2. Compound **39** reversed the position of the cinnamyl group and placed it into pocket 1, with the dimethyl aniline group in pocket 2. This led to increased potency but decreased selectivity. The cinnamyl group of compound **53** again docked into pocket 2, whereas the 8-aminoquinoline group docked into the smaller, narrower pocket 3. These results seemed to suggest that pocket 2 was important for selectivity and, in combination with pocket 3, enhanced both potency and selectivity in this series of compounds. Design of future compounds that target all three pockets may provide a series of compounds with even greater potency and selectivity.

Cytoselectivity. Several compounds from Table 1 exhibited selectivity in their cell killing of MM96L melanoma cells versus normal NFF cells. Compounds that displayed ≥ 5 -fold selectivity were **6**, **15–18**, **24**, **26**, **29**, **33**, **37**, **42**, **44–46**, **51–53**, and **55**. Compounds **52** and **55** were > 10 -fold more selective, compound **51** was > 20 and compound **53** was nearly 60 times more selective in killing MM96L cells over NFF cells. This represents a significant > 10 -fold increase in selectivity of cell killing over our previous best cysteine-derived compounds.²⁶ Based on these antiproliferative and cytoselective properties, we further tested

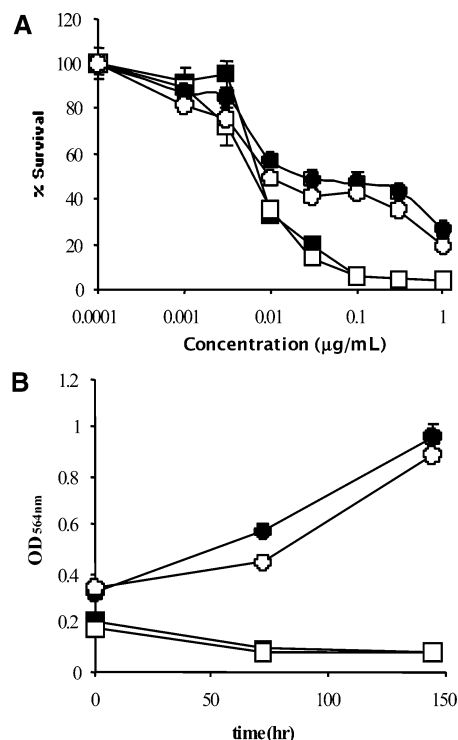


Figure 3. Cytoselectivity and Cell Regrowth. MM96L metastatic melanoma (squares) or NFF (circles) cells were treated with **52** (open symbols) or **53** (closed symbols) for 24 h before removal of the compounds. (A) Cells were allowed to grow for 3 days before assay of clonogenic survival. (B) Cells were assayed immediately after removal of the compounds and at 72 and 144 h following to examine cell regrowth.

compounds **16**, **47**, **50–52**, **54**, and **55** against a panel of other human cancer cell lines (Tables 2 and 3).

Compound **16** was found to be potent ($IC_{50} < 1 \mu M$) against 16 melanoma cell lines and very potent ($IC_{50} \leq 0.1 \mu M$) against seven of these melanoma cells (MM329, MM470, MM604, Mel RM, SK-Mel-28, D17, and A2058). This derivative was also moderately selective (SI 10–15-fold) for four melanomas (MM329, Mel FH, SK-Mel-28, and D17) and very selective (SI 87) for the MM604 melanoma cell line. Compound **16** was also very potent (90 nM) against the cervical carcinoma HeLa cells and moderately selective (SI 9.7) over normal NFF cells.

Six derivatives (**47**, **51–53**, **55**, and **56**) were tested for potency and cytoselectivity against a range of 14 cell lines,

Table 3. Antiproliferative Potency (IC_{50} , μM) and Cytoselectivity (SI) for Compounds **47**, **51–53**, **55**, and **56** Against Cancer Cell Lines^a

cell line	47		51		52		53		55		56	
	IC ₅₀ (μM)	SI	IC ₅₀ (μM)	SI	IC ₅₀ (μM)	SI	IC ₅₀ (μM)	SI	IC ₅₀ (μM)	SI	IC ₅₀ (μM)	SI
NFF	0.185		0.570		0.337		1.240		0.452		0.081	
A549	0.335	0.6	0.148	3.9	0.069	4.9	0.073	17.0	0.248	1.8	0.291	0.3
DU145	0.149	1.2	0.061	9.4	0.022	15.2	0.030	40.8	0.131	3.4	0.130	0.6
HOP62	0.261	0.7	0.137	4.2	0.063	5.3	0.065	19.0	0.226	2.0	0.267	0.3
HT29	0.307	0.6	0.178	3.2	0.079	4.3	0.099	12.5	0.334	1.4	0.360	0.2
MCF-7	0.149	1.2	0.035	16.3	0.019	17.7	0.017	71.3	0.122	3.7	0.138	0.6
MM96L	0.121	1.5	0.051	11.1	0.018	18.8	0.020	63.4	0.056	8.0	0.116	0.7
SK-MEL-28	0.168	1.1	0.073	7.8	0.033	10.3	0.037	33.6	0.146	3.1	0.170	0.5
SK-MEL-5	0.102	1.8	0.032	17.6	0.018	18.2	0.029	43.1	0.070	6.5	0.100	0.8
H520	0.117	1.6	0.063	9.1	0.026	12.8	0.027	45.7	0.118	3.8	0.129	0.6
T-47D	0.197	0.9	0.045	12.7	0.019	17.7	0.020	63.4	0.093	4.9	0.198	0.4
CI80-13S	0.158	1.2	0.065	8.8	0.020	16.8	0.028	43.9	0.124	3.6	0.149	0.5
JAM	0.182	1.0	0.085	6.7	0.048	7.1	0.049	25.4	0.194	2.3	0.221	0.4
PC-3	0.531	0.3	0.220	2.6	0.148	2.3	0.109	11.4	0.528	0.9	0.651	0.1
Colo205	0.272	0.7	0.223	2.5	0.102	3.3	0.141	8.7	0.122	3.7	0.395	0.2

^a A549 (lung), DU145 (prostate), HOP62 (lung), HT29 (colon), MCF7 (breast), MM96L (melanoma), SK-MEL-28 and SK-MEL-5 (melanoma), Colo205 (colon), CI80-13S (ovarian), JAM (ovarian), H520 (lung), T47D (breast), and PC-3 (prostate).

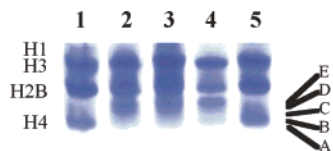


Figure 4. Acetylation of histones following treatment with compounds. MM96L cells were treated with DMSO alone (lane 1), **16** (at 0.05, 0.5, or 5 $\mu\text{g}/\text{mL}$, lanes 2–4, respectively), or no treatment (lane 5) for 8 h. Histones were extracted and analyzed by TAU gel electrophoresis. Shown are nonacetylated (A), monoacetylated (B), diacetylated (C), triacetylated (D), and tetraacetylated (E) histone H4.

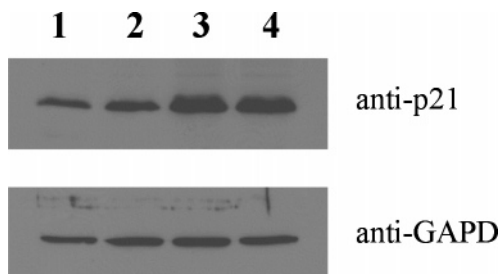


Figure 5. Induction of p21 expression. A549 cells were treated with **52** for 24 h and protein extracted from cells. Protein (30 μg) was subjected to western blot analysis using antibodies specific for p21^{WAF1/Cip1} and GAPD. Lane 1, vehicle only; lane 2, 0.05 $\mu\text{g}/\text{mL}$; lane 3, 0.5 $\mu\text{g}/\text{mL}$; and lane 4, 5 $\mu\text{g}/\text{mL}$.

including melanoma, lung, prostate, colon, ovarian, and breast cancers (Table 3). These compounds were all potent anticancer drugs with IC_{50} values $< 1 \mu\text{M}$ for all cancer types tested. In particular, compounds **52** and **53** had $\text{IC}_{50} < 20 \text{ nM}$ against MM96L, SK-Mel-5 (melanomas), MCF-7, T-47D (breast), CI80-13S (ovarian), and MCF-7, MM96L, respectively. Compound **52** was generally the more potent but with only 18-fold selectivity over the normal cells, whereas **53** was slightly less potent but shows better selectivity over normal cells (at least twice that of **52**, i.e., $\text{SI} \geq 40$), being in some cases greater than three times more selective than compound **52** (i.e., MCF-7 ($\text{SI} = 71.3$), MM96L ($\text{SI} = 63.4$), and T-47D ($\text{SI} = 63.4$)). Compounds **47**, **51**, and **55** show good anticancer potency against a range of cell lines but with more modest cytoselectivities for cancer cells over normal cells ($\text{SI} < 18$) compared to that of **52** and **53**. Compound **56** was also potent against cancer cells, but lacked selectivity, possibly due to a smaller nonaromatic group at the R^1 position.

It was observed, when measuring the antiproliferative potency of the compounds, that the normal cells NFF rarely showed complete cell death. This was indicated by relatively high absorbance readings following clonogenic cell survival assays, approximately 30% of untreated cells (Figure 3A). In contrast,

MM96L cells show almost complete killing by the compounds tested, as indicated by very low absorbance values ($< 5\%$ of untreated cells; Figure 3A). To further investigate this, a regrowth assay was performed. Both MM96L and NFF cells were treated with 0.3 $\mu\text{g}/\text{mL}$ of **52** or **53** for 24 h. The compounds were then removed, and cells were either fixed immediately or allowed to grow for a further 72 or 144 h. The MM96L cells were unable to maintain any further growth even after 6 days, indicating that all cells were dead or nonproliferating following a 24 h treatment (Figure 3B). In contrast, NFF cells showed growth as evidenced by an increase in staining with sulfarhodamine B following removal of the compounds. The increase in growth is most likely due to the cell cycle block induced in normal cells by similar compounds.³⁵ Given that the normal NFF cells that are being released from the cell cycle block are still rapidly growing, it is probable that the cytoselectivity value (SI) indicated for the compounds is an underestimation. The selectivity of this class of compounds for cancer cells compared to normal cells is possibly more stringent.

Histone Hyperacetylation. Illustrative of histone hyperacetylation experiments conducted on the above compounds, Figure 4 shows that compound **16** induces hyperacetylation of histones, consistent with inhibiting HDACs. The increase in hyperacetylated histones was found to be dose-dependent (Figure 4), consistent with results observed with HDAC inhibitors reported elsewhere.¹⁹

p21 Expression. Expression of p21 was examined following treatment with compound **52** (Figure 5). Induction of p21 was observed in all cell lines examined, including the normal NFF cells (data not shown) and A549 lung adenocarcinoma cells (Figure 5). The metastatic melanoma cell line MM96L, which has very low constitutive expression of p21, showed a minimal increase in expression (data not shown). It has been reported that cells that do not up-regulate p21 are hypersensitive to apoptotic killing by HDAC inhibitor compounds.³⁶ However, it is clear that the increase in p21 expression is not limited to either normal or cancer cells.

Morphological Reversion. Malignancy is often associated with a phenotype characterized by morphological distortion of normal cytoskeleton and cell shape. Compounds that can revert the transformed morphology of malignant cells to that of a normal phenotype may be valuable new classes of antitumor drugs. For example, hydroxamic acid **6**, like many of the compounds herein, was found to induce dramatic changes in cellular shape in MM96L cells, photographed after a 24 h treatment with 3 $\mu\text{g}/\text{mL}$ of the drug (Figure 6). Compound **6** profoundly alters the spherical morphology of surviving melanoma cells, making them more dendritic like normal melano-



Figure 6. Morphological transformation after 24 h. (left) Untreated melanoma cells (MM96L); (right) MM96L treated with **6** (3 $\mu\text{g}/\text{mL}$) for 24 h.

cytes. We have reported this result before for HDAC inhibitors like ABHA⁷ and cysteine-derived²⁶ anticancer compounds.

Conclusions

Histone deacetylase inhibitors can arrest growth and induce differentiation and/or apoptotic cell death in a variety of human and normal cancer cell lines, with histones becoming hyperacetylated in both normal and cancer cells. Known HDAC inhibitors do not appear to discriminate in their inhibition of HDAC enzymes between normal and cancer cells. While there is a need for new inhibitors that are selective for individual HDACs to distinguish their possibly specific roles in cell proliferation, broader spectrum HDAC inhibitor pharmacophores might also be useful, but in another way for evolving more tumor-selective compounds even if HDACs themselves are not the origin of cytospecific anticancer activity. Conceivably, the antiproliferative, apoptotic, and differentiating properties of HDAC inhibitors could be dissected and separately enhanced for more specific and more selective drug action on cancer cells.

Herein we have reported a series of compounds, designed and synthesized from α -aminosuberic acid, that have potent cytotoxicity for cancer cell lines. The homology structure of the enzyme was used extensively to guide the selection of fragments for our parallel synthesis library. There was a strong emphasis on small hydrophobic groups, and several basic groups were chosen to mimic dimethylaniline but without protonation *in vivo*. We also considered interactions with either the Lys or Glu at the entrance to the HDAC active site. The basic groups in particular appear to have conferred both potency and selectivity to the anticancer properties of the compounds. Indeed, **51**, which presumably interacts using both of these features, is quite potent.

A few of these compounds differed from our previously reported cysteine-derived series²⁶ by only a simple replacement of $-S-$ by $-CH_2-$ and also incorporated a much more diverse, but still focused, combinatorial series of N- and C-terminal substituents to α -aminosuberic acid. For the limited set of compounds where direct structural comparisons can be made, the cytotoxicity comparisons do not show a clear trend. For example, compounds **18**, **28**, and **29** are respectively >30-, 5-, and 3-fold *more* potent, and 7-, 1-, and 2-fold *more* selective, than the corresponding analogues derived from cysteine (**21**, **29**, and **20** in ref 26) in killing MM96L melanoma cells over NFF cells; whereas compounds **6**, **25**, **26**, and **33** are respectively 10-, 10-, 2-, and 3-fold *less* potent but about equally as selective as their corresponding analogues derived from cysteine (**9**, **11**, **35**, and **27** in ref 26). Such comparisons are presumably compromised by the variable cooperativity of enzyme–ligand interactions, the length of the linker to hydroxamate differentially affecting the fitting of R¹/R² substituents to the indentations in the enzyme surface surrounding the entrance to the active site.

Thus, while more potent (10–100-fold greater) and selective (up to 10-fold higher) killing of cancer cells (e.g., MCF-7, T-47D, and MM96L) over normal cells (e.g., NFF) has been documented for this compound series versus our previous observations for cysteine-derived anticancer compounds,²⁶ we cannot say that the suberoyl analogues are always more potent and selective as a class than **3** or **4**. Moreover, the selectivity that has been observed herein was not maintained for all cancer cell lines tested. Also, while the series was based on inhibiting HDAC enzymes, demonstrated through assays for hyperacetylation of histones, induction of p21 expression, and selective morphological reversion of tumor cells, the enhanced selectivity for compounds in this paper is not attributed to HDAC

inhibition. We have previously reported that ABHA triggers a G2 checkpoint in normal cells that is defective in tumor cells,³⁵ and this is an important factor in comparing selectivities for normal versus cancer cells.

There are also a number of chemical and biological advantages for suberoyl compounds over the cysteine derived thioether group. Chemically, the thioether sulfur is a well-known pi-acceptor that can coordinate strongly to metal ions, thereby also potentially directing the previously reported²⁶ compounds to other proteins/enzymes/metals, leading to biological properties (side effects) not possible for suberoyl analogues with no metal-binding sulfur. The thioether can also be readily oxidized to sulfoxide, then to sulfone, and participate in free-radical chemistry; such redox chemistry is not possible for suberoyl compounds. Metabolically, compounds containing the thioether sulfur would also be more likely to be lost in first pass metabolism through oxidative degradation by cytochrome P450 enzymes in the liver and GI tract.

Further optimization at the N-, C-, and S-termini of α -aminosuberic or related scaffolds could provide a great deal of scope for generating compounds with greater potency and selectivity through more effective interactions with HDACs or other cellular targets. Also, one might consider replacing the hydroxamate moiety,³⁷ a general metal-binding ligand that may negatively impact on clinical properties similar to problems encountered with matrix metalloproteinase inhibitors as a result of nonselective metal binding. Such enhancements are expected to make this class of compounds more effective molecular probes, not only for interactions with the HDAC family of enzymes, but also for other cellular targets that may be responsible for the possibly separate pharmacophores that contribute to cytotoxicity, cytospecificity, and phenotypic reversion.

Experimental Methods

General Methods. ¹H NMR spectra were recorded on a Bruker Avance 600 MHz, a Bruker ARX 500 MHz, or a Varian 300 MHz NMR spectrometer. Semipreparative scale rpHPLC separations were performed on a Phenomenex Luna 5 μ C18(2) 250 \times 21 mm column run at 20 mL/minute using gradient mixtures of water/0.1% TFA (A) and water (10%)/acetonitrile (90%)/0.1% TFA (B), and product fractions were always lyophilized to dryness. Preparative scale rpHPLC separations were performed on a Vydac 218TP101550 50 \times 250 mm column run at 70 mL/minute using gradient mixtures of A and B. Accurate mass determinations were performed on an API QSTAR mass spectrometer using electron impact ionization. Water octanol partition coefficients (log *D*) were predicted using PALLAS prolog D 2.1. Molecular modeling was performed on an SGI Octane R12000, with minimization calculations performed with the cff91 force field using the Discover Module within InsightII.

Homology Model. A homology model was generated for HDAC1 based on the structure of the bacterial homologue HDLP. Sequences of class 1 HDACs (HDAC1–3, 8) were aligned with HDLP and correlated against the structure (secondary structure prediction). The HDAC1 model was generated by assigning coordinates of HDAC1 residues (and HDAC2) based on the mainchain of HDLP. This was used to identify residues potentially important for binding around the shallow, solvent-exposed pocket adjacent to the entrance to the active site channel. No further refinement was carried out due to the flexible nature of loops around the active site. Model building was carried out using the homology module within the InsightII modeling suite.³⁸ All calculations were carried out on an R10,000 work station.

Ligand Docking. InsightII was used to construct the required inhibitors (TSA, Trapoxin and **6**) in preparation for flexible docking using the GOLD program. Ligands were then flexibly docked into the active site of the HDAC1 homology model using GOLD with

a standard parameter setup. GOLD generated ten docked conformations for each ligand and ranked their relative binding conformations.

Chemical Synthesis. A parallel synthesis library of compounds was constructed from a few key synthesized reagents as follows.

6-Iodo-hexanoic Acid *tert*-Butyl Ester: 6-Bromo-hexanoic acid (10 g, 51.3 mmol) was dissolved in 1,4-dioxane (30 mL) in a pressure vessel and cooled in a dry ice/acetone bath. Isobutylene (30 mL) was added to the solution, followed by H₂SO₄ (0.5 mL). The vessel was closed and the mixture was stirred at rt for 48 h before it was poured into a separatory funnel with satd NaHCO₃ (aq; 150 mL) and extracted with diethyl ether (3 × 150 mL). The combined organic phase was washed with brine (2 × 150 mL). The organic phase was dried (MgSO₄), and the volatiles were removed under vacuum. The resulting oil was dissolved in THF (200 mL), NaI (30.7 g, 205 mmol) was added to the reaction flask, and the mixture was refluxed for 16 h. The reaction was cooled to rt, and the volume of solvent was reduced under vacuum, and diethyl ether (300 mL) was added to the solution, resulting in salt precipitation. The salt was filtered off with a sintered funnel, and the solvent was poured into a separation funnel and washed with brine (2 × 200 mL). The organic phase was dried (MgSO₄), evaporated, and purified by chromatography (petroleum ether/EtOAc, 9:1) to give a yellow oil in 90% yield over two steps. ¹H NMR (CDCl₃, 600 MHz) δ 3.18 (t, *J* = 7.0 Hz, 2H), 2.21 (t, *J* = 7.5 Hz, 2H), 1.79–1.85 (m, 2H), 1.56–1.62 (m, 2H), 1.43 (s, 9H), 1.40–1.43 (m, 4H); ¹³C NMR (CDCl₃, 125 MHz) δ 173.1, 80.3, 35.4, 33.3, 30.0, 28.3, 28.3, 28.3, 24.1, 7.1.

2-Acetylamino-2-ethoxycarbonyl-octanedioic Acid 8-*tert*-Butyl Ester 1-Ethyl Ester: NaH (60% dispersion in mineral oil; 3.97 g, 99.1 mmol) was added to a solution of diethyl acetamidomalonate **7** (19.57 g, 90.1 mmol) dissolved in DMF (150 mL). After 30 min, iodo-hexanoic acid *tert*-butyl ester (30 g, 117.2 mmol) was added to the mixture, and the solution was stirred at rt for 4 h. The reaction mixture was poured into a separatory funnel, extracted with diethyl ether (3 × 150 mL), and washed with brine (2 × 150 mL). The organic phase was dried (MgSO₄), evaporated, and purified by chromatography (petroleum ether/EtOAc, 3:1) to give a yellow oil in 93% yield. ¹H NMR (CDCl₃, 600 MHz) δ 6.77 (br s, 1H), 4.23 (q, *J* = 7.1 Hz, 4H), 2.29–2.32 (m, 2H), 2.16 (t, *J* = 7.2 Hz, 2H), 2.03 (s, 3H), 1.52–1.57 (m, 2H), 1.42 (s, 9H), 1.28–1.33 (m, 2H), 1.24 (t, *J* = 7.1 Hz, 6H), 1.08–1.13 (m, 2H); ¹³C NMR (CDCl₃, 125 MHz) δ 173.2, 169.1, 168.4, 80.2, 66.7, 62.7, 60.6, 35.5, 32.2, 28.9, 28.3, 25.1, 23.6, 23.2, 14.2.

2-Acetylamino-octanedioic Acid 8-*tert*-Butyl Ester 1-Ethyl Ester: LiCl·H₂O (622 mg, 14.5 mmol) and H₂O (347 μL, 19.3 mmol) were added to a solution of 2-acetylamino-2-ethoxycarbonyl-octanedioic acid 8-*tert*-butyl ester 1-ethyl (3.736 g, 9.64 mmol) dissolved in DMSO (50 mL). The mixture was heated to 150 °C for 16 h, extracted with diethyl ether (3 × 100 mL), and washed with brine (2 × 100 mL). The organic phase was dried (MgSO₄), evaporated, and put on high vacuum for 10 h to give the product in 98% yield as a yellow oil. ¹H NMR (CDCl₃, 600 MHz) δ 6.08 (d, *J* = 7.7 Hz, 1H), 4.55–4.59 (m, 1H), 4.19 (q, 4H, *J* = 7.3 Hz), 2.18 (t, *J* = 7.6 Hz, 2H), 2.01 (s, 3H), 1.79–1.84 (m, 2H), 1.62–1.67 (m, 2H), 1.53–1.58 (m, 2H), 1.42 (s, 9H), 1.28–1.33 (m, 2H), 1.27 (t, 3H, *J* = 7.2 Hz); ¹³C NMR (CDCl₃, 125 MHz) δ 173.2, 172.9, 170.0, 80.2, 61.6, 52.3, 35.5, 32.6, 28.8, 28.3, 28.3, 25.0, 25.0, 23.4, 14.3.

2-Acetylamino-octanedioic Acid 8-*tert*-Butyl Ester (8): LiOH·H₂O (1.79 g, 42.5 mmol) was added to 2-acetylamino-octanedioic acid 8-*tert*-butyl ester 1-ethyl ester (8.93 g, 28.4 mmol) dissolved in 100 mL of H₂O/EtOH (1:1). The pH was made neutral by citric acid (aq) after about 1 h, and the EtOH was removed by evaporation. The solution was poured into a separatory funnel, extracted with EtOAc (3 × 150 mL), and washed with brine (2 × 150 mL). The organic phase was dried (MgSO₄), evaporated, and purified by chromatography (petroleum ether/EtOAc, 1:1) to give a pale yellow oil in 93% yield. ¹H NMR (CDCl₃, 600 MHz) δ 6.30 (d, *J* = 7.3 Hz, 1H), 4.56–4.61 (m, 1H), 2.22 (t, *J* = 7.4 Hz, 2H), 2.06 (s, 3H), 1.87–1.93 (m, 1H), 1.64–1.76 (m, 3H), 1.55–

1.62 (m, 2H), 1.45 (s, 9H), 1.30–1.38 (m, 2H); ¹³C NMR (CDCl₃, 151 MHz) δ 175.3, 173.4, 170.9, 80.3, 52.3, 35.3, 31.7, 28.5, 28.1, 24.8, 24.7, 23.0.

2-(9H-Fluoren-9-ylmethoxycarbonylamino)-octanedioic Acid 8-*tert*-Butyl Ester (10): This compound has been reported before and has been enzymatically resolved using *Aspergillus* amino acylase-I to produce the pure *S*-enantiomer, which has a well-established optical³⁹ and NMR spectral data. This enzyme has also been used to resolve similar acids.^{40,41} An alternative is to resolve D,L-2-aminosuberlic acid using papain-catalyzed ester hydrolysis,⁴² which we now prefer for preparing this class of compounds.

Acetylamino-octanedioic acid 8-*tert*-butyl ester (7.5 g, 26.2 mmol) was dissolved in phosphate buffer (0.1 M, pH 7.2, 500 mL), and the pH was adjusted to 7.2 by the addition of 2 M NaOH. The resulting solution was warmed to 39 °C, and CoCl₂·6H₂O (75 mg) was added with gentle shaking. Acylase I (*Aspergillus melleus*, 375 mg) was added to the solution, and the reaction was left to sit for up to 48 h at 39 °C. This is a well-established approach to enzymatic resolution of the racemic intermediate. Although the 2*S*-enantiomer is selectively deacetylated initially, experiments lasting over 24 h tended to produce some 2*R*-enantiomer, even though its Ac derivative is deacetylated at a substantially reduced rate.

Analysis of an aliquot of the solution by ¹H NMR indicated a 1:1 mixture of the amine and the acetamide. The solvent was removed to about half the volume by evaporation and 250 mL of THF was added. NaHCO₃ (4.4 g, 52.4 mmol) and Fmoc-succinate (4.6, 13.7 mmol) was added to the solution, and the mixture was stirred for 2 h. The solvent was removed under reduced pressure, and the residue was suspended in EtOAc (300 mL) and washed successively with water, 1 M HCl, saturated NaHCO₃ solution, and brine. The organic layer was dried (MgSO₄), evaporated, and purified by chromatography (petroleum ether/EtOAc, 2:1) to give a pale yellow oil in 45% yield. ¹H NMR (CDCl₃, 600 MHz) δ 7.77 (d, *J* = 7.5 Hz, 2H), 7.61 (m, 2H), 7.41 (dd, *J* = 7.4 Hz, 2H), 7.32 (dd, *J* = 7.4, 7.3 Hz, 2H), 5.33 (d, *J* = 8.2 Hz, 1H), 4.38–4.45 (m, 3H), 4.23 (t, *J* = 7.0 Hz, 1H), 3.92 (br s, 1H), 2.22 (t, *J* = 7.4 Hz, 2H), 1.88–1.92 (m, 1H), 1.69–1.73 (m, 1H), 1.59–1.62 (m, 2H), 1.45 (s, 9H), 1.35–1.44 (m, 4H); ¹³C NMR (CDCl₃, 151 MHz) δ 176.4, 173.6, 156.3, 143.9, 141.5, 128.0, 127.4, 125.3, 120.2, 80.5, 67.3, 53.8, 47.4, 35.6, 32.3, 28.7, 28.3, 25.1, 24.9. The *S*-enantiomer of Fmoc-Asu(*Or*-*Bu*)-OH has a well-established optical rotation [α]_D –16.9 deg (0.51 g/100 mL, DMF, 22 °C).³⁹ Alternatively, the papain-catalyzed hydrolysis of Z-D,L-Asu(OMe)-OMe, followed by hydrolysis with methanolic NaOH, affords the different derivatives of the *S*-enantiomer, Z-L-Asu-OH ([α]_D –9.1 deg, DMF) and *R*-enantiomer, Z-D-Asu-OH ([α]_D +9.1 deg, DMF), as described.⁴²

2-(9H-Fluoren-9-ylmethoxycarbonylamino)-octanedioic Acid 1-Allyl Ester 8-*tert*-Butyl Ester (11): Allyl bromide (1.74 g, 14.4 mmol) was added in one portion to a suspension of NaHCO₃ (4.4 g, 52.4 mmol) and ester **10** (5.5 g, 11.8 mmol) in DMF (200 mL). The resulting solution was stirred for 30 min, and then the solvent was removed under reduced pressure. The resulting residue was dissolved in EtOAc (500 mL) and washed successively with water and brine (2 × 200 mL). The organic layer was dried (MgSO₄), and the solvent was removed under reduced pressure to provide the title allyl ester as a yellow oil in 92% yield. ¹H NMR (CDCl₃, 600 MHz) δ 7.78 (d, *J* = 7.6 Hz, 2H), 7.60–7.62 (m, 2H), 7.41 (dd, 2H, *J* = 7.5 Hz), 7.33 (dd, *J* = 7.5 Hz, 2H), 5.91–5.93 (m, 1H), 5.27–5.37 (m, 2H), 4.66 (br s, 2H), 4.40–4.42 (m, 3H), 4.24 (t, *J* = 7.1 Hz, 1H), 2.21 (t, *J* = 7.5 Hz, 2H), 1.85–1.90 (m, 1H), 1.67–1.73 (m, 1H), 1.56–1.62 (m, 2H), 1.45 (s, 9H), 1.31–1.40 (m, 4H); ¹³C NMR (CDCl₃, 151 MHz) δ 173.2, 172.5, 156.1, 144.1, 144.0, 141.5, 131.7, 127.9, 127.3, 125.9, 120.2, 119.2, 80.3, 67.2, 66.2, 54.1, 47.4, 35.6, 32.7, 28.8, 28.3, 25.1, 25.0.

2-(9H-Fluoren-9-ylmethoxycarbonylamino)-octanedioic Acid 1-Allyl Ester: *tert*-Butyl ester **11** (4.0 g, 7.83 mmol) was stirred in 9:1 TFA/DCM (50 mL) for 30 min. The solvent was removed under reduced pressure, and the residue was purified by flash chromatography (petroleum ether/EtOAc, 2:1) to provide the title acid as a white solid in 89% yield. ¹H NMR (CDCl₃, 600 MHz) δ

7.78 (d, $J = 7.6$ Hz, 2H), 7.60–7.62 (m, 2H), 7.41 (dd, $J = 7.5$ Hz, 2H), 7.33 (dd, $J = 7.4$ Hz, 2H), 5.91–5.93 (m, 1H), 5.27–5.37 (m, 2H), 4.66 (br s, 2H), 4.41–4.42 (m, 3H), 4.24 (t, $J = 7.0$ Hz, 1H), 2.35 (t, $J = 7.4$ Hz, 2H), 1.86–1.88 (m, 1H), 1.63–1.70 (m, 3H), 1.26 = 7–1.42 (m, 4H); ^{13}C NMR (DMSO, 125 MHz) δ 179.1, 172.3, 155.9, 143.8, 143.7, 141.3, 131.4, 127.7, 127.0, 125.0, 119.9, 118.9, 67.0, 65.9, 53.8, 47.1, 33.7, 32.4, 28.5, 24.8, 24.3.

Coupling of Acid to Resin (12). Commercially available *N*-Fmoc hydroxylamine 2-chlorotriptyl resin (0.77 mmol/g, 7.54 g, 5.81 mmol) was shaken gently with 1:1 piperidine/DMF (20 mL) overnight and then washed through with DMF 10 times. In a separate flask, HATU (2.26 g, 6.10 mmol) was added to a solution of 2-(9*H*-fluoren-9-ylmethoxycarbonylamino)-octanedioic acid 1-allyl ester (3.14 g, 7.0 mmol) and DIPEA (5.06 mL, 29.0 mmol) dissolved in DMF (10 mL), and the resulting solution was stirred gently for 10 min. The HATU-activated acid was then added in one portion to the deprotected resin, and the resin was shaken gently for 1 h. After washing the resin well with DMF, the resin loading of **12** was determined to be 0.522 mmol/g (91%; LRMS *m/e* calcd for $\text{C}_{26}\text{H}_{30}\text{N}_2\text{O}_6$ (MH⁺), 467.2; found, 467.2). The unreacted resin was then acylated by addition of a solution of acetic anhydride (842 mg, 7.8 mmol) and DIPEA (5.3 mL, 31.2 mmol) in DMF (20 mL) with shaking for 2 min, followed by thorough washing with DMF.

Removal of the Allyl Ester: The resin was flow washed with DCM for 2 min and then shaken in DCM (30 mL) for a further 10 min. A nitrogen stream was introduced, and the resin and DCM were degassed for 5 min. DMBA (0.80 g, 5.12 mmol) was added, and bubbling was continued for a further minute to ensure thorough mixing. Pd(Ph₃)₄ (493 mg, 0.43 mmol) was added to the resin and the flask was wrapped in aluminum foil, and after a further 30 s of degassing, the nitrogen stream was removed, and the resin was shaken gently for 1 h. The resin was flow washed successively with DCM, DMF, and DCM before drying under high vacuum. (LRMS *m/e* calcd for $\text{C}_{23}\text{H}_{26}\text{N}_2\text{O}_6$ (MH⁺), 427.2; found, 427.1).

Coupling of Amines General Procedure (13): The resin was shaken in DMF for 10 min, and then DIPEA (5 equiv) and 0.5 M HBTU in DMF (1.1 equiv) were introduced and shaking continued for a further 5 min. The desired amine (1 equiv) was then added, and shaking was continued for a further 1 h. After washing the resin well with DMF, cleavage of a small portion of resin, and analysis by mass spectroscopy generally indicated 40–85% conversion to the amide. Repeating the coupling provides increased conversion.

Coupling of Acids General Procedure (14): The resin was shaken in DMF for 10 min, the DMF removed, and then 1:1 piperidine/DMF added. After shaking for 5 min, the piperidine/DMF was removed, and the resin was washed well with DMF. This procedure was repeated two more times. In a separate flask, 0.5 M HBTU (4 equiv) in DMF was added to a solution of the desired acid (4 equiv) and DIPEA (16 equiv) in DMF (1 mL), and the resulting solution was stirred for 5 min before being added in one portion to the resin. The resin was shaken for 1 h, and then washed well with DMF. Cleavage of a small portion of resin and analysis by mass spectroscopy generally indicates 100% conversion to the amide.

General Procedure for Cleavage of the Product from Resin: The resin was washed well with DCM and then drained. TFA/DCM (95:5) with a drop of water (per 50 mL) was added, and the resin was shaken for 20 min. The TFA was collected, and the procedure was repeated 1–2 more times. The solvent was removed by evaporation. Purification was performed by rpHPLC, and hydroxamates were confirmed to be greater than 95% pure by analytical rpHPLC and ^1H NMR spectroscopy. All hydroxamic acids displayed high field ^1H NMR spectral and HRMS parameters consistent with their proposed structures, with nine relevant examples shown.

Hydroxamic Acid 24. ^1H NMR (acetone-*d*₆, 500 MHz) δ 10.76 (s, 2H), 9.93 (s, 1H), 7.87 (t, $J = 6.0$ Hz, 1H), 7.81 (d, $J = 8.0$ Hz, 1H), 7.61 (d, $J = 8.0$ Hz, 1H), 7.3–7.1 (m, 5H), 7.06 (t, $J = 8$ Hz, 1H), 4.64 (m, 1H), 4.42 (d, $J = 6$ Hz, 2H), 4.39 (s, 1H), 1.96 (m,

2H), 1.80 (m, 2H), 1.60 (m, 2H), 1.4–1.3 (m, 4H); ^{13}C NMR (DMSO-*d*₆, 75 MHz) δ 171.9, 169.1, 161.1, 139.5, 136.4, 131.3, 128.2, 127.0, 126.7, 123.4, 121.5, 119.7, 112.2, 109.5, 53.1, 42.0, 32.2, 31.6, 28.3, 25.5, 25.0; HRMS calcd for $\text{C}_{29}\text{H}_{33}\text{N}_3\text{O}_4$ (MH⁺), 488.2544; found, 488.2527.

Hydroxamic Acid 25. ^1H NMR (acetone-*d*₆, 500 MHz) δ 9.92 (s, 2H), 7.88 (d, $J = 8.5$ Hz, 2H), 7.84 (d, $J = 6.5$ Hz, 2H), 7.65 (d, $J = 8.5$ Hz, 2H), 7.28 (m, 3H), 7.21 (m, 1H), 4.62 (m, 1H), 4.42 (d, $J = 6$ Hz, 2H), 2.72 (s, 1H), 1.94 (m, 2H), 1.79 (m, 2H), 1.58 (m, 2H), 1.4–1.3 (m, 4H); ^{13}C NMR (DMSO-*d*₆, 75 MHz) δ 171.8, 169.1, 165.6, 139.5, 133.3, 131.2, 129.7, 128.2, 127.0, 126.7, 125.0, 53.7, 42.0, 32.2, 31.5, 28.3, 25.5, 25.0; HRMS calcd for $\text{C}_{22}\text{H}_{26}\text{BrN}_3\text{O}_4$ (MH⁺), 476.1179; found, 476.1200.

Hydroxamic Acid 28. ^1H NMR (acetone-*d*₆, 500 MHz) δ 9.91 (s, 1H), 7.80 (s, 1H), 7.68 (m, 2H), 7.64 (d, $J = 7.5$ Hz, 2H), 7.57 (d, $J = 8.2$ Hz, 2H), 7.46–7.38 (m, 5H), 7.35–7.20 (5H), 4.44 (m, 1H), 4.37 (d, $J = 6.0$ Hz, 2H), 3.62 (d, $J = 4.2$ Hz, 2H), 1.81 (m, 2H), 1.62 (m, 2H), 1.53 (m, 2H), 1.30 (m, 4H); ^{13}C NMR (DMSO-*d*₆, 75 MHz) δ 171.7, 170.0, 169.1, 140.0, 139.4, 138.2, 135.8, 129.6, 128.9, 128.2, 127.3, 127.0, 126.7, 127.1, 126.7, 126.5, 126.4, 52.6, 41.9, 41.7, 32.2, 32.1, 28.3, 25.1, 25.0; HRMS calcd for $\text{C}_{29}\text{H}_{33}\text{N}_3\text{O}_4$ (MH⁺), 488.2544; found, 488.2527.

Hydroxamic Acid 31. ^1H NMR (DMSO-*d*₆, 600 MHz) δ 10.31 (s, 1H), 8.40 (s, 1H), 7.41 (d, $J = 8.1$ Hz, 2H), 7.36–7.29 (m, 6H), 7.23 (d, $J = 7.5$ Hz, 2H), 5.02 (d, $J = 3.5$ Hz, 2H), 4.27 (dd, $J = 5.6, 3.7$ Hz, 2H), 3.97 (m, 1H), 3.44 (br s, 1H), 1.91 (t, $J = 7.4$ Hz, 2H), 1.69 (m, 1H), 1.56 (m, 1H), 1.45 (m, 2H), 1.31–1.23 (m, 4H); ^{13}C NMR (DMSO-*d*₆, 75 MHz) δ 172.0, 169.0, 168.1, 139.4, 137.1, 128.3, 128.2, 127.8, 127.7, 127.0, 127.7, 65.3, 54.7, 42.0, 32.2, 31.8, 28.3, 25.2, 25.0; HRMS calcd for $\text{C}_{23}\text{H}_{29}\text{N}_3\text{O}_5$ (MH⁺), 428.2180; found, 428.2209.

Hydroxamic Acid 32. ^1H NMR (DMSO-*d*₆, 600 MHz) δ 10.31 (s, 1H), 8.52 (t, $J = 7.2$ Hz, 1H), 8.1 (d, $J = 8.1$ Hz, 2H), 7.85 (d, $J = 8.2$ Hz, 2H), 7.64 (br s, 1H), 7.32–7.22 (m, 5H), 4.40 (m, 1H), 4.28 (d, $J = 7.2$ Hz, 2H), 1.91 (t, $J = 7.5$ Hz, 2H), 1.77 (m, 2H), 1.47 (m, 2H), 1.37–1.26 (m, 4H); ^{13}C NMR (DMSO-*d*₆, 75 MHz) δ 171.7, 169.0, 165.4, 139.5, 137.9, 128.5, 128.2, 127.0, 126.7, 125.2, 125.1, 53.8, 42.0, 32.2, 31.4, 28.3, 25.5, 25.0; HRMS calcd for $\text{C}_{23}\text{H}_{26}\text{F}_3\text{N}_3\text{O}_4$ (MH⁺), 466.1948; found, 466.1968.

Hydroxamic Acid 50. ^1H NMR (DMSO-*d*₆, 600 MHz) δ 10.31 (s, 1H), 8.25 (d, $J = 8.4$ Hz, 1H), 8.16 (d, $J = 7.2$ Hz, 1H), 7.35 (m, 2H), 7.29 (m, 2H), 7.13 (m, 3H), 5.03 (m, 2H), 4.94 (m, 1H), 3.97 (m, 1H), 2.71 (m, 2H), 1.91 (t, $J = 7.5$ Hz, 2H), 1.84 (m, 2H), 1.69–1.54 (m, 4H), 1.45 (m, 2H), 1.31–1.23 (m, 4H); HRMS calcd for $\text{C}_{26}\text{H}_{31}\text{N}_5\text{O}_4$ (MH⁺), 478.2456; found, 478.2449.

Hydroxamic Acid 51. ^1H NMR (DMSO-*d*₆, 600 MHz) δ 10.54 (s, 1H), 10.32 (s, 1H), 8.78 (d, $J = 4.3$ Hz, 1H), 8.65 (m, 3H), 8.42 (dd, $J = 8.3, 1.6$ Hz, 1H), 7.86 (d, $J = 9.0$ Hz, 1H), 7.66 (dd, $J = 8.3, 1.2$ Hz, 1H), 7.60 (dd, $J = 8.3, 4.2$ Hz, 1H), 7.58 (t, $J = 8.0$ Hz, 1H), 6.7 (d, $J = 9.0$ Hz, 2H), 4.61 (m, 1H), 1.93 (t, $J = 7.5$ Hz, 2H), 1.49 (m, 2H), 1.48–1.45 (m, 2H), 1.31–1.23 (m, 4H); HRMS calcd for $\text{C}_{26}\text{H}_{31}\text{N}_5\text{O}_4$ (MH⁺), 478.2456; found, 478.2449.

Hydroxamic Acid 52. ^1H NMR (DMSO-*d*₆, 600 MHz) δ 11.65 (s, 1H), 10.52 (s, 1H), 10.32 (s, 1H), 8.99 (d, $J = 7.4$ Hz, 1H), 8.78 (m, 1H), 8.65 (dd, $J = 7.9, 1.1$ Hz, 1H), 8.64 (s, 1H), 8.39 (dd, $J = 8.3, 1.6$ Hz, 1H), 7.69–7.66 (m, 2H), 7.60–7.57 (m, 2H), 7.43 (d, $J = 8.3$ Hz, 1H), 7.39 (s, 1H), 7.20 (t, $J = 7.9$ Hz, 1H), 7.06 (t, $J = 7.8$ Hz, 1H), 4.72 (m, 1H), 1.93 (t, $J = 7.3$ Hz, 2H), 1.50 (m, 4H), 1.48–1.30 (m, 4H); ^{13}C NMR (DMSO-*d*₆, 125 MHz) δ 170.8, 169.0, 161.7, 148.8, 137.8, 136.5, 133.9, 130.8, 127.7, 126.9, 126.9, 123.5, 122.1, 121.9, 121.6, 119.7, 116.0, 112.2, 107.5, 103.7, 54.5, 32.2, 30.6, 28.3, 25.5, 24.9; HRMS calcd for $\text{C}_{26}\text{H}_{27}\text{N}_5\text{O}_4$ (MH⁺), 474.2148; found, 474.2136.

Hydroxamic Acid 53. ^1H NMR (DMSO-*d*₆, 600 MHz) δ 10.46 (s, 1H), 10.31 (s, 1H), 8.86 (dd, $J = 4.3, 1.7$ Hz, 1H), 8.64 (dd, $J = 7.7, 1.3$ Hz, 1H), 8.41 (dd, $J = 8.3, 1.7$ Hz, 1H), 8.31 (dd, $J = 8.5, 3.6$ Hz, 1H), 7.69 (dd, $J = 8.3, 1.3$ Hz, 1H), 7.59–7.55 (m, 2H), 7.50 (d, $J = 15.8$ Hz, 1H), 7.65 (dd, $J = 8.3, 4.2$ Hz, 1H), 7.59 (t, $J = 8.0$ Hz, 1H), 7.44–7.7.39 (m, 3H), 6.84 (d, $J = 15.8$ Hz, 1H), 4.11 (m, 1H), 1.93 (t, $J = 7.5$ Hz, 2H), 1.64–1.58 (m, 2H), 1.46 (m, 2H), 1.34–1.27 (m, 4H); ^{13}C NMR (DMSO-*d*₆, 125

MHz) δ 170.7, 169.0, 165.5, 148.9, 139.5, 137.9, 136.5, 134.7, 133.9, 129.5, 128.9, 127.7, 127.5, 126.9, 122.1, 121.9, 121.3, 116.1, 54.4, 32.1, 31.0, 28.2, 25.2, 24.9; HRMS calcd for $C_{26}H_{28}N_4O_4$ (MH⁺), 461.2174; found, 461.2184.

Cell Lines and Culture Medium. All cell lines used in this study have been described previously.^{43,44} All cell lines were cultured in 10% heat-inactivated fetal calf serum (CSL, Australia) in RPMI 1640 medium supplemented with 100 U/mL penicillin, 100 μ g/mL streptomycin, and 3 mM HEPES at 5% CO₂, 99% humidity at 37 °C. Primary human fibroblasts were obtained from neonatal foreskins and cultured in the above medium. Routine mycoplasma tests were performed using Hoechst stain⁴⁵ and were always negative.

Cell Survival Assay. Cells were plated into 96-well microtitre plates at 5×10^3 cells/well and allowed to adhere overnight. Compounds were added to culture medium at the indicated concentrations, and the plates were incubated in the above conditions for 24 h. Following this incubation period, compounds and media were removed and replaced with fresh culture medium. Cells were then grown for a further 72 h before assay using sulforhodamine B (SRB; Sigma, St. Louis, MO), as previously described.^{46,47} Briefly, the culture medium was removed from the 96-well microtitre plates, and the plates were washed twice with phosphate-buffered saline (PBS) before the cells were fixed with methylated spirits for 15 min. The plates were then rinsed with tap water, and the fixed cells were stained with 50 μ L/well of SRB solution (0.4% sulforhodamine B (w/v) in 1% (v/v) acetic acid) over a period of 1 h. The SRB solution was then removed from the wells, and the plates were rapidly washed two times with 1% (v/v) acetic acid. Protein-bound dye was then solubilized with the addition of 100 μ L of 10 mM unbuffered Tris and incubated for 15 min at 25 °C. Plates were then read at 564 nm on a VERSA max tuneable microplate reader (Molecular Devices, Sunnyvale, CA).

Analysis Following Treatment. Clonogenic cell survival following treatment with compounds, morphological reversion, and analysis of histone hyperacetylation were all performed as previously described.²⁶

Generation of Total Cell Lysates, Gel Electrophoresis, and Immunoblotting. Total cell lysates from 1×10^7 cells were generated by sonication (60 pulses) in 200 μ L of lysis buffer (20% glycerol, 1% SDS, 10 mM Tris-HCl pH 7.4, 1 \times complete protease inhibitor (Roche)), and then centrifuged at 15 000 \times g for 15 min to obtain a soluble protein fraction. Samples were stored at -70 °C until use. Protein concentration was measured with the BCA protein assay (Pierce, Rockford, IL) using bovine serum albumin as a standard. Samples (30 μ g protein) were resolved by 15% SDS-polyacrylamide gel electrophoresis and transferred to nitrocellulose membranes. Visualization of the p21 or GAPD proteins was by an anti-p21 antibody (1 in 1000 dilution; Transduction Laboratories,) or anti-GAPD antibody (1 in 10 000 dilution; R&D Systems, Minneapolis, MN), followed by an anti-mouse or anti-rabbit (Chemicon, Melbourne, Australia) IgG-horse radish peroxidase-conjugated secondary antibody, respectively, and renaissance chemiluminescent detection (NEN Life Science Products, Boston, MA) using Kodak X-OMAT AR 18 \times 24 cm film and developed with a Kodak X-Omat developer.

Histone Hyperacetylation. Analysis of histone H4 acetylation by triton-acetic acid-urea gel was carried out as previously described.³⁵

Acknowledgment. We thank the Australian Research Council, Australian National Health and Medical Research Council, and The Hans Werthén Foundation for some financial support.

Supporting Information Available: Mass spectral and HPLC data. This material is available free of charge via the Internet at <http://pubs.acs.org>.

References

- Rodriguez, M.; Aquino, M.; Bruno, I.; De Martino, G.; Taddei, M.; Gomez-Paloma, L. Chemistry and biology of chromatin remodelling agents: state of art and future perspectives of HDAC inhibitors. *Curr. Med. Chem.* **2006**, *13*, 1119–1139.
- (a) Marks, P. A.; Richon, V. M.; Kiyokawa, H.; Rifkind, R. A. Inducing differentiation of transformed cells with hybrid polar compounds: a cell cycle-dependent process. *Proc. Natl. Acad. Sci. U.S.A.* **1994**, *91*, 10251–10254. (b) Rifkind, R. A.; Richon, V. M.; Marks, P. A. Induced differentiation, the cell cycle and the treatment of cancer. *Pharmacol. Ther.* **1996**, *69*, 97–102.
- Leszczyniecka, M.; Roberts, T.; Dent, P.; Grant, S.; Fisher, P. B.; Differentiation, therapy of human cancer: basic science and clinical implications. *Pharmacol. Ther.* **2001**, *90*, 105–156.
- (a) Lin, H. Y.; Chen, C. S.; Lin, S. P.; Weng, J. R.; Chen, C. S. Targeting histone deacetylase in cancer therapy. *Med. Res. Rev.* **2006**, *26*, 397–413. (b) Vigushin, D. M.; Coombes, R. C. Histone deacetylase inhibitors in cancer treatment. *Anti-Cancer Drugs* **2002**, *13*, 1–13.
- Marks, P. A.; Rifkind, R. A.; Richon, V. M.; Breslow, R.; Miller, T.; Kelly, W. K. Histone deacetylases and cancer: causes and therapies. *Nature* **2001**, *1*, 194–202.
- Richon, V. M.; Emiliani, S.; Verdin, S.; Webb, Y.; Breslow, R.; Rifkind, R. A.; Marks, P. A. A class of hybrid polar inducers of transformed cell differentiation inhibits histone deacetylases. *Proc. Natl. Acad. Sci. U.S.A.* **1998**, *95*, 3003–3007.
- (a) Parsons, P. G.; Hansen, C.; Fairlie, D. P.; West, M. L.; Danoy, P. A. C.; Sturm, R. A.; Dunn, I. S.; Pedley, J.; Ablett, E. M. Tumor selectivity and transcriptional activation by azalaic bishydroxamic acid in human melanocytic cells. *Biochem. Pharmacol.* **1997**, *53*, 1719–1724. (b) Qui, L.; Kelso, M. J.; Hansen, C.; West, M. L.; Fairlie, D. P.; Parsons, P. G. Antitumor activity in vitro and in vivo of selective differentiating agents containing hydroxamate. *Br. J. Cancer* **1999**, *80*, 1252–1258.
- (a) Butler, L. M.; Agus, D. B.; Sher, H. I.; Higgins, B.; Rose, A.; Cordon-Cardo, C.; Thaler, H. T.; Rifkind, R. A.; Marks, P. A.; Richon, V. M. Suberoylanilide hydroxamic acid, an inhibitor of histone deacetylase, suppresses the growth of prostate cancer cells in vitro and in vivo. *Cancer Res.* **2000**, *60*, 5165–5170. (b) Kelly, W. K.; Marks, P. A. Drug insight: Histone deacetylase inhibitors—development of the new targeted anticancer agent suberoylanilide hydroxamic acid. *Nat. Clin. Pract. Oncol.* **2005**, *2*, 150–157.
- (a) Su, G. H.; Sohn, T. A.; Ryu, B.; Kern, S. E. A novel histone deacetylase inhibitor identified by high-throughput transcriptional screening of a compound library. *Cancer Res.* **2000**, *60*, 3137–3142. (b) Varghese, S.; Gupta, D.; Baran, T.; Jiemjit, A.; Gore, S. D.; Casero, R. A., Jr.; Woster, P. M. Alkyl-substituted polyaminohydroxamic acids: A novel class of targeted histone deacetylase inhibitors. *J. Med. Chem.* **2005**, *48*, 6350–6365.
- Tsuji, N.; Kobayashi, M.; Nagashima, K.; Wakisaka, Y.; Koizumi, K. A new antifungal antibiotic, trichostatin. *J. Antibiot.* **1976**, *29*, 1–6.
- Yoshida, M.; Kijima, M.; Akita, M.; Beppu, T. Potent and specific inhibition of mammalian histone deacetylase both in vivo and in vitro by trichostatin A. *J. Biol. Chem.* **1990**, *265*, 17174–17179.
- Kijima, M.; Yoshida, M.; Sugita, K.; Horinouchi, S.; Beppu, T. Trapoxin, an antitumor cyclic tetrapeptide, is an irreversible inhibitor of mammalian histone deacetylase. *J. Biol. Chem.* **1993**, *268*, 22429–22435.
- Darkin-Rattray, S. J.; Gurnett, A. M.; Myers, R. W.; Dulski, P. M.; Crumley, T. M.; Allocco, J. J.; Cannova, C.; Meinke, P. T.; Colletti, S. L.; Bednarek, M. A.; Singh, S. B.; Goetz, M. A.; Dombrowski, A. W.; Polishook, J. D.; Schmatz, D. M. Apicidin: a novel antiprotozoal agent that inhibits parasite histone deacetylase. *Proc. Natl. Acad. Sci. U.S.A.* **1996**, *93*, 13143–13147.
- Yoshida, M.; Furumai, R.; Nishiyama, M.; Komatsu, Y.; Nishino, N.; Horinouchi, S. Histone deacetylase as a new target for cancer chemotherapy. *Cancer Chemother. Pharmacol.* **2001**, *48*, S20–S26.
- Furumai, R.; Komatsu, Y.; Nishino, N.; Khochbin, S.; Yoshida, M.; Horinouchi, S. Potent histone deacetylase inhibitors built from trichostatin A and cyclic tetrapeptide antibiotics including trapoxin. *Proc. Natl. Acad. Sci. U.S.A.* **2001**, *98*, 87–92.
- Murray, P. J.; Kranz, M.; Laddow, M.; Taylor, S.; Berst, F.; Holmes, A. B.; Keavey, K. N.; Jaxa-Chamiec, A.; Seale, P. W.; Stead, P.; Upton, R. J.; Croft, S. L.; Clegg, W.; Elsegood, M. R. J. The synthesis of cyclic tetrapeptide analogues of the antiprotozoal natural product Apicidin. *Bioorg. Med. Chem. Lett.* **2001**, *11*, 773–776.
- (a) Taunton, J.; Collins, J. L.; Schreiber, S. L. Synthesis of natural and modified trapoxins, useful reagents for exploring histone deacetylase function. *J. Am. Chem. Soc.* **1996**, *118*, 10412–10422. (b) Komatsu, Y.; Tomizaki, K.; Tsukamoto, M.; Kato, T.; Nishino,

- N.; Sato, S.; Yamori, T.; Tsuruo, T.; Furumai, R.; Yoshida, M.; Horinouchi, S.; Hayashi, H. Cyclic hydroxamic-acid-containing peptide 31, a potent synthetic histone deacetylase inhibitor with antitumor activity. *Cancer Res.* **2001**, *61*, 4459–4460.
- (18) (a) Marson, C. M.; Savy, P.; Rioja, A. S.; Mahadevan, T.; Mikol, C.; Veerupillai, A.; Nsubuga, E.; Chahwan, A.; Joel, S. P. Aromatic sulfide inhibitors of histone deacetylase based on arylsulfanyl-2,4-hexadienoic acid hydroxyamides. *J. Med. Chem.* **2006**, *49*, 800–805. (b) Lu, Q.; Wang, D. S.; Chen, C. S.; Hu, Y. D.; Chen, C. S. Structure-based optimization of phenylbutyrate-derived histone deacetylase inhibitors. *J. Med. Chem.* **2005**, *48*, 5530–5535.
- (19) Atadja, P.; Gao, L.; Kwon, P.; Trogani, N.; Walker, H.; Hsu, M.; Yeleswarapu, L.; Chandramouli, N.; Perez, L.; Versace, R.; Wu, A.; Sambucetti, L.; Lassota, P.; Cohen, D.; Bair, K.; Wood, A.; Remiszewski, S. Selective growth inhibition of tumor cells by a novel histone deacetylase inhibitor, NVP-LAQ824. *Cancer Res.* **2004**, *64*, 689–695.
- (20) Gregoret, I. V.; Lee, Y. M.; Goodson, H. V. Molecular evolution of the histone deacetylase family: Functional implications of phylogenetic analysis. *J. Mol. Biol.* **2004**, *338*, 17–31.
- (21) De Ruijter, A. J. M.; Van Gennip, A. H.; Caron, H. N.; Kemp, S. Van Kuilenburg, A. B. P. Histone deacetylases (HDACs): Characterization of the classical HDAC family. *Biochem. J.* **2003**, *370*, 737–749.
- (22) Finnin, M. S.; Donigian, J. R.; Cohen, A.; Richon, V. M.; Rifkind, R. A.; Marks, P. A.; Breslow, R.; Pavletich, N. P. Structures of a histone deacetylase homologue bound to the TSA and SAHA inhibitors. *Nature* **1999**, *401*, 188–193.
- (23) Somoza, J. R.; Skene, R. J.; Katz, B. R.; Mol, C.; Ho, J. D.; Jennings, A. J.; Luong, C.; Arvai, A.; Buggy, J. J.; Chi, E.; Tang, J.; Sang, B. C.; Verner, E.; Wynands, R.; Leahy, E. M.; Dougan, D. R.; Snell, G.; Navre, M.; Knuth, M. W.; Swanson, R. V.; McRee, D. E.; Tari, L. W. Structural snapshots of human HDAC8 provide insights into the class I histone deacetylases. *Structure* **2004**, *12*, 1325–1334.
- (24) Vannini, A.; Volpari, C.; Filocamo, G.; Casavola, E. C.; Brunetti, M.; Renzoni, D.; Chakravarty, P.; Paolini, C.; De Francesco, R.; Gallinari, P.; Steinkühler, C.; Di Marco, S. Crystal structure of a eukaryotic zinc-dependent histone deacetylase, human HDAC8, complexed with a hydroxamic acid inhibitor. *Proc. Natl. Acad. Sci. U.S.A.* **2004**, *101*, 15064–15069.
- (25) Wegener, D.; Hildmann, C.; Schwienhorst, A. Recent progress in the development of assays for histone deacetylase inhibitor screening. *Mol. Genet. Metab.* **2003**, *80*, 138–147.
- (26) Glenn, M. P.; Kahnberg, P.; Boyle, G. M.; Hansford, K. A.; Hans, D.; Martyn, A. C.; Parsons, P. G.; Fairlie, D. P. Antiproliferative and phenotype-transforming antitumor agents derived from cysteine. *J. Med. Chem.* **2004**, *47*, 2984–2994.
- (27) Grozinger, C. M.; Schreiber, S. L. Deacetylase enzymes: biological functions and the use of small-molecule inhibitors. *Chem. Biol.* **2002**, *9*, 3–16.
- (28) Kao, H. Y.; Lee, C. H.; Komarov, A.; Han, C. C.; Evans, R. M. Isolation and characterization of mammalian HDAC10, a novel histone deacetylase. *J. Biol. Chem.* **2002**, *277*, 187–193.
- (29) Gao, L.; Cueto, M. A.; Asselbergs, F.; Atadja, P. Cloning and functional characterization of HDAC11, a novel member of the human histone deacetylase family. *J. Biol. Chem.* **2002**, *277*, 25748–25755.
- (30) Gregoret, I. V.; Lee, Y. M.; Goodson, H. V. Molecular evolution of the histone deacetylase family: functional implications of phylogenetic analysis. *J. Mol. Biol.* **2004**, *338*, 17–31.
- (31) (a) G. Jones, G.; Willett, P.; Glen, R. C.; Leach, A. R.; Taylor, R. Development and validation of a genetic algorithm for flexible docking. *J. Mol. Biol.* **1997**, *267*, 727–748. (b) Verdonk, M. L.; Cole, J. C.; Hartshorn, M. J.; Murray, C. W.; Taylor, R. D. Improved protein-ligand docking using GOLD. *Proteins* **2003**, *52*, 609–623.
- (32) Mohamadi, F.; Richards, N. G. J.; Guida, W. C.; Liskamp, R.; Lipton, M.; Caufield, C.; Chang, G.; Hendrickson, T.; Still, W. C. MacroModel—an integrated software system for modeling organic and bioorganic molecules using molecular mechanics. *J. Comput. Chem.* **1990**, *11*, 440–467.
- (33) Glenn, M. P.; Kelso, M. J.; Tyndall, J. D. A.; Fairlie, D. P. Conformationally homogeneous cyclic tetrapeptides: useful three dimensional scaffolds. *J. Am. Chem. Soc.* **2003**, *125*, 640–641.
- (34) Tsantili-Kakoulidou, A.; Panderi, I.; Csizmadia, F.; Darvas, F. Prediction of distribution coefficient from structure. 2. Validation of prolog D, and expert system. *J. Pharm. Sci.* **1997**, *86* (10), 1173–1179.
- (35) Qiu, L.; Burgess, A.; Fairlie, D. P.; Leonard, H.; Parsons, P. G.; Gabrielli, B. G. Histone deacetylase inhibitors trigger a G2 checkpoint in normal cells that is defective in tumor cells. *Mol. Biol. Cell* **2000**, *11*, 2069–2083.
- (36) Burgess, A. J.; Pavey, S.; Warrener, R.; Hunter, L. J.; Piva, T. J.; Musgrove, E. A.; Saunders, N.; Parsons, P. G.; Gabrielli, B. G. Up-regulation of p21(WAF1/CIP1) by histone deacetylase inhibitors reduces their cytotoxicity. *Mol. Pharmacol.* **2001**, *60*, 828–837.
- (37) Curtin, M. L. Synthesis of novel hydroxamate and non-hydroxamate histone deacetylase inhibitors. *Curr. Opin. Drug Discovery Dev.* **2004**, *7*, 848–868.
- (38) Accelrys, Inc. *InsightII Modeling Environment*, release 2000; Accelrys, Inc.: San Diego, CA, 2001.
- (39) Hlavacek, J.; Marcova, R.; Budesinsky, M. 1-deamino-1(15)-carba and -dicarba analogues of endothelin-1. *Collect. Czech. Chem. Commun.* **2000**, *65*, 407–424.
- (40) Greenstein, J. P.; Birnbaum, S. M.; Otey, M. C. Optical enantiomers of α -amino adipic acid. *J. Am. Chem. Soc.* **1953**, *75*, 1994–1995.
- (41) Mori, K.; Sugai, T.; Maeda, Y.; Okazaki, T.; Noguchi, T.; Naito, H. Synthesis of the racemic and optically active forms of gizzerosine, the inducer of gizzard erosion in chicks. *Tetrahedron* **1985**, *41*, 5307–5311.
- (42) Rivard, M.; Malon, P.; Cerovsky, V. Resolution of D,L-2-aminosuber acid via protease-catalysed ester hydrolysis. *Amino Acids* **1998**, *15*, 389–392.
- (43) Parsons, P. G.; Bowman, E. P. W.; Blakely, R. L. Selective toxicity of deoxyadenosine analogues in human melanoma cell lines. *Biochem. Pharmacol.* **1986**, *35*, 4025–4029.
- (44) Todaro, G. J.; Fryling, C.; De Larco, J. E. Transforming growth factors produced by certain human tumour cells: polypeptides that interact with epidermal growth factor receptors. *Proc. Natl. Acad. Sci. U.S.A.* **1980**, *77*, 5258–5262.
- (45) Chen, T. R. In situ detection of mycoplasma contamination in cell cultures by fluorescent Hoechst 33258 stain. *Exp. Cell. Res.* **1977**, *104*, 255–262.
- (46) Skehan, P.; Storeng, R.; Scudiero, D.; Monks, A.; McMahon, J.; Vistica, D.; Warren, J. T.; Bokesch, H.; Kenney, S.; Boyd, M. R. New colorimetric cytotoxicity assay for anticancer-drug screening. *J. Natl. Cancer Inst.* **1990**, *82*, 1107–1112.
- (47) Rubinstein, L. V.; Shoemaker, R. H.; Paull, K. D.; Simon, R. M.; Tosini, S.; Skehan, P.; Scudiero, D. A.; Monks, A.; Boyd, M. R. Comparison of in vitro anticancer-drug-screening data generated with a tetrazolium assay versus a protein assay against a diverse panel of human tumor cell lines. *J. Natl. Cancer Inst.* **1990**, *82*, 1113–1118.

JM050214X